MODELLING AND SIMULATION OF A FULLY ELECTRIC HYBRID PROPULSION SYSTEM FOR PASSENGER SHIPS USING AVL CRUISE-M SOFTWARE

LUCA MICOLI[1], ROBERTA RUSSO[1], TOMMASO COPPOLA[1], AND DANIELE SEVERI[2]

[1]Department of Industrial Engineering, University of Naples Federico II
Via Claudio, 21, 80125, Naples, Italy
luca.micoli@unina.it

[1]Department of Industrial Engineering, University of Naples Federico II
Via Claudio, 21, 80125, Naples, Italy
tomcoppo@unina.it

[1]Department of Industrial Engineering, University of Naples Federico II
Via Claudio, 21, 80125, Naples, Italy
roberta.russo5@unina.it

[2]AVL Italia S.R.L.
Corso Francesco Ferrucci, 112, 10138, Turin, Italy
daniele.severi@avl.com

Key words: Maritime transport, PEM fuel cell, hydrogen, multi-physic simulation.

Abstract. The maritime industry's pursuit of sustainability drives the exploration of alternative fuels, with hydrogen emerging as a promising solution. This paper presents a comprehensive study on a fully electric hybrid propulsion system for passenger ships, utilizing hydrogen as the primary power source. Multi-physics simulation using AVL Cruise-M software enables detailed analysis of system dynamics and performance. Results from a full acceleration test reveal the intricate interplay between the fuel cell and battery system, crucial for meeting power demands during transient phases. Examination of material flows highlights the importance of maintaining optimal water balance for system efficiency and durability. Temperature and pressure variations significantly influence FC efficiency, showcasing improvements over time, stabilizing at approximately 56% efficiency after 2.6 minutes. These findings underscore the value of comprehensive simulations and temporal analysis in optimizing hybrid propulsion systems, suggesting strategies for further enhancement, such as precise temperature and mass flow control.

1 INTRODUCTION

In today's maritime industry, the focus on sustainability has reached new heights, leading to increased efforts in seeking alternative fuels to address environmental concerns. The urgent need to curb carbon emissions and reduce reliance on conventional fuels has sparked a significant transition towards greener and more efficient technology solutions. Various

alternatives such as hydrogen, biofuels, ammonia, and methanol have the potential to achieve this goal, as stated by the International Maritime Organization (IMO), whose initiatives are aimed at reducing greenhouse gas emissions (GHG) from ships [1].

Shipbuilders improve energy efficiency by either reducing hull resistance or enhancing the fuel efficiency of propulsion systems. However, zero-emission vessels will ultimately need electrification and green energy, highlighting the need for sustainable solutions. Numerous electrically propelled ships utilizing motor drives have been developed. Ongoing studies in the realm of electric propulsion ships focus on electric control systems or motor drives [2,3]. However, research regarding the electricity source remains limited. In most current vessels, electricity is generated through the combustion of fuels with diesel generators or gas turbine generators, which are far from environmentally friendly. Consequently, various researchers have investigated the sustainability of electric propulsion ships.

Fully electric zero-emission vessels, equipped with secondary batteries, have been developed utilizing both batteries and fuel cells as sources of electricity for ships [4–6].Batteries are generally confined primarily to small ships for coastal or inland operations due to energy capacity limitations and recharging inconvenience. The use of fuel cells appears more feasible mainly in terms of energy densities, but there are some issues related to fuel storage [7]. Numerous studies and projects focusing on hydrogen-fueled ships have explored hybrid ship propulsion systems, which integrate polymer electrolyte membrane fuel cells (PEMFC) with lithium-ion battery systems [8–12]. The PEMFC system is gaining attentions as a viable power generating system for ships due to its high-power density, rapid start-up capabilities, and lower operating temperatures compared to other devices and fuel cell types. A PEMFC is fuelled by pure hydrogen and air. Hydrogen (H_2) stands out as a promising option for the maritime sector due to its potential for zero emissions. It has the highest gravimetric energy density (33.31 kWh/kg), on the other hand, its volumetric energy density is relatively low. Therefore, to enhance storage density, it is typically stored either as a compressed gas (up to 700 bad) or a liquid (at -253 °C) [13]. Hydrogen, as an environmentally friendly fuel, holds huge promise for tackling the challenges posed by traditional marine propulsion systems.

Among the most effective strategies to meet stringent emissions standards is the replacement of conventional internal combustion vehicles with Hybrid Electric Vehicles (HEVs) which integrate an electric motor powered by a rechargeable battery alongside a FC system for power generation, utilizing hydrogen stored onboard as an energy carrier. This hybridization enables HEVs to seamlessly switch between electric motor and conventional engine usage, resulting in improved fuel efficiency and reduced emissions [14]. Moreover, the integration of hybrid powertrains, which combine hydrogen technologies with other energy sources and storage systems, offers a strategic method to improve efficiency and address certain constraints of standalone H_2 systems. This blending enhances versatility and reliability in power solutions for maritime purposes. The examination of these hybrid setups contributes to a comprehensive exploration of sustainable propulsion strategies for ships.

In this context, multi-physics simulations streamline the development of fully electric propulsion systems by modelling various physical phenomena simultaneously. Engineers utilize these simulations to optimize designs, predict performance, and ensure safety and reliability. By analysing transient behaviour and assessing environmental impact, simulations aid in creating efficient and sustainable propulsion solutions. These tools enable iterative design

refinement, minimizing costs and development time while maximizing system efficiency and effectiveness [15].

According to this, the study outlined in this paper concentrates on the modelling of a fully electric hybrid propulsion system for a passenger ship using AVL Cruise-M multi-physics simulation software. Specifically, the powertrain integrates a Proton Exchange Membrane Fuel Cell (PEMFC), a battery pack, an electric motor, and all related auxiliary devices, utilizing compressed hydrogen as the primary power source.

2 METHODOLOGY

2.1 Multi-physics simulation

Cruise-M is a multi-disciplinary system simulation solution supporting model-based development with real-time models from various domains: engine, flow, aftertreatment, driveline, electrics, hydraulics, etc. It efficiently handles multi-physics system simulation through a flexible, multi-level modeling approach. Multi-physics multi-rate co-simulation splits the numerical solution of system models into multiple circuits, benefiting simulation times by employing dedicated numerical solution methods and time-step sizes for individual circuits. Non-stiff circuits, like thermal networks, can use larger step sizes compared to stiff circuits, such as electrical networks.

In Cruise-M, multi-physics simulation enables different solvers and settings per physical domain and circuit, decomposing the Differential Algebraic Equation (DAE) system into several DAEs representing physical circuits:

$$x'_i = f_i(t, x_i, y_i) \quad (1)$$

$$0 = g_i(t, x_i, y_i) \quad (2)$$

where, t is the time; x_i is the system state; and y_i is the algebraic variables.

Therefore, Electric, fluid, and gas circuits have separate DAEs, while other circuits (i.e. rotational mechanics, translational mechanics, thermal, waste heat recovery) are combined into the main DAE. Summarizing, the whole model can be broken down to

- *n* gas circuits,
- *n* electric circuits,
- *n* fluid liquid circuits,
- one main circuit.

For each circuit one arbitrary solver can be parametrized. Therefore, the maximal number of parametrized solvers is:

$$n = n_{gas} + n_{electric} + n_{liquid} + 1 \quad (3)$$

In general, each circuit can be parametrized with any solver settings, though restrictions may apply due to the physical domain's nature.

The solver parametrization process involves three parts:

1. Parametrizing solver settings for the main circuit similar to single-rate parametrization.
2. Assigning solver settings to corresponding circuits in each domain (fluid, electric, gas).
3. Individually parametrizing all assigned solver settings (solver type, time-step type, step size, and solver).

Information exchange between solvers occurs at a synchronization time step Δt_s, with each solver adjusting its individual step size Δt_i to match Δt_s.

Implicit solvers typically allow larger time steps than explicit solvers, with the Jacobian system often calculated via finite differences. Hence, for larger systems and mildly stiff problems, it is more efficient to use explicit plus adaptive solvers instead of implicit solvers. If the model gives an Ordinary Differential Equations (ODE), CVODE is used [16], while IDA is used for Differential Algebraic Equations (DAE)[17]. Both use Backward Difference Formulas (BDF) with inner steps, error estimation and order adaptations. For details see [16] and [17].

For explicit solvers, the selection of fixed, auto or adaptive for time stepping is possible. All variants include event handling, which is needed, for example, for the proper clutch closing.

Cruise-M employs a subset of solvers with different orders, including one-step Runge-Kutta methods with internal stages for explicit solvers. Details about the stages and the Butcher tables can be found in [18]. Assuming sufficient smoothness in the system, the methods have the following numerical integration error order:

- Euler, order 1
- Heun, order 2
- Bogacki/Shampine, order 3
- ARK-4, order 3
- Zonneveld, order 4

Different methods also have an embedded error estimator, like Bogacki-Shampine, which is utilized for the step size control. Methods of the same order have different stability regions [18], hence, if one fails, the other with the same computational effort may run without problems.

The smoothness of the system influences solver selection, with Heun and Bogacki-Shampine generally sufficient for most applications. Different methods offer varying numerical integration error orders and stability regions, ensuring robustness and efficiency across simulations.

2.2 Model

The hybrid power plant propulsion model, illustrated in Figure 1, comprises several subsystems, units, and their interconnections, briefly described as follows.

The propeller subsystem (PS) incorporates mathematical models for the ship's resistance and kinematics. Specific ship performance evaluations, including total resistance and effective power at the required speed, considering full load conditions and weight distribution, can be imported from other software, such as full-scale URANS simulations. Performance data and efficiencies at the design speed are integrated and considering the required effective power, also the propeller’s specifics can be considered.

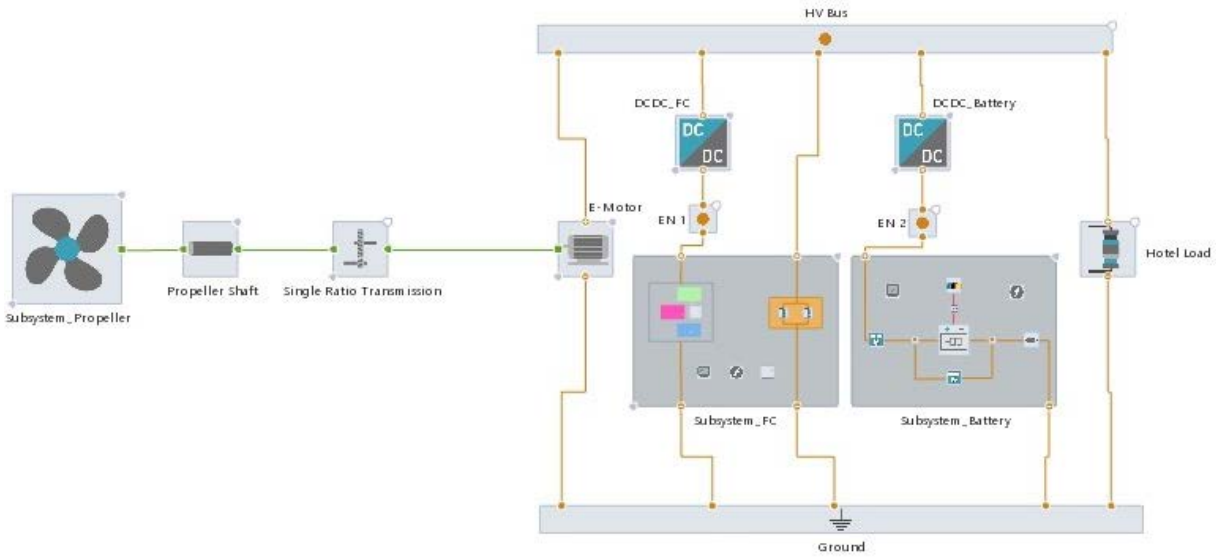

Figure 1: Scheme of the hybrid power plant propulsion

The electric motor (EM) subsystem features an electric machine model. Initially, it delivers the requested torque, which can be either the specified torque or the equivalent torque derived from the full load characteristic and requested mechanical load. Subsequently, power losses are added to the delivered mechanical power to obtain the electrical power. Alternatively, the electrical power can be directly calculated using the efficiency map definition and the delivered mechanical power. Depending on the relevant property, either the efficiency map or power losses map is defined for the machine and inverter (if present), individually for each active quadrant. This definition process mirrors that of the full load characteristics. These maps serve as references for interpolating losses on the component, utilizing four dimensions: temperature, voltage, rotor speed, and torque (or mechanical power). In the present model, the EM has a maximum efficiency value of 96% at 1600 rpm and 500 V, corresponding to a torque of 4639 Nm and mechanical power of 777 kW. The EMS drives the PS through a transmission and shaft unit and is connected to the main switchboard of the ship at 500 V.

The Fuel Cell (FC) model separately accounts for the components of the Proton Exchange Membrane (PEM) and its Balance of Plant (BoP), such as cathode air supply, water and thermal management, power conditioning, etc. The FC model includes the following subsystems:

1. FC stacks subsystem model: Features a 1D resolution along the gas channel flow and a reduced dimensionality electrochemical model. The model comprises multiple cells with variable geometry, along with other physical and chemical specifics that users can customize or select from the software's library. Users can also implement a single-cell performance characterized by a polarization curve. The FC stack model simulates the relevant thermodynamic, electrochemical, and transport processes occurring within the FC as a function of the chosen components' materials.

2. Anode subsystem (AS): Models the H_2 flow at the anode FC section, including a recirculation branch of unused humid hydrogen that is fed back through a Venturi injector. Excess water from the anode gas outflow is removed by a water separator to maintain constant humidity. A PID is used to control the Venturi injector opening and regulate the pressure. The

AS also includes the H_2 tank subsystem, which comprises a tank plenum supplemented with a charging valve restriction, a discharging valve restriction, a relief device valve restriction, and a relief device control function.

3. Cathode subsystem (CS): Consists of a compressor, capable of providing up to ~0.5 kg/s of external air pumped up to 4 bar. The compressed air is cooled down and then circulated through the humidifier component before reaching the FC stack to provide the desired humidity to the membrane. Pressure and airflow are regulated via two PID controllers that control the compressor and the backpressure valve.

4. Thermal management subsystem (TMS): Simulates a cooling circuit that uses environmental water to exchange heat. Circulation in the TMS is driven by a pump regulated considering the heat flow generated by the FC system with a correction provided by a PID to maintain the FC temperature at a constant value. It is assumed that the FC has already reached the operating temperature (70 °C), allowing a faster response to transient loads.

5. The battery subsystem (BS): Consists of a controlled voltage source and an Ohmic resistance used to describe the instantaneous voltage response to a current input. It includes an advanced model to predict the transient voltage response to a dynamic current load, eventually coupled with a thermal model to predict the transient thermal behavior of the battery. The BS comprises battery packs made of multiple cells connected in series and parallel with a battery management system (BMS) for peak and continuous power. It serves as recuperation storage, as a buffer when the FC system is active, and as the main storage when the power request is below the activation threshold of the FC system. The BS can be specifically designed according to the case study ship and operating routing profile, for instance, varying the initial State of Charge (SoC), the operating voltage, and the single-cell configuration (series-parallel). Open circuit voltage and Ohmic resistance variations as functions of the SoC are implemented, assuming common trends for Li-ion-based batteries. During normal operation, the battery is charged towards 90% of SoC. If power demand rises too quickly or exceeds the maximum rated power of the FC subsystem, the battery covers the remainder.

As the EM, FC stacks, and BS operate within different voltage ranges, two DC-DC converter units are considered to boost the voltages up to the E-Motor side level. It is supposed that both the DC-DC converters have an efficiency of 93%.

3 RESULTS

Results of the multi-physics simulation are presented in Figures 2- 4 considering a full acceleration test to investigate the power-generating subsystems' responses with a ship speed ranging from 0 to 13 knots in 5 minutes.

Figure 2 illustrates the variation in FC and BS power responses corresponding to the total load demand during the acceleration test. The load demand primarily comprises the EM power request, the air compressor, the pump, and the hotel load, with the latter assumed to remain constant at 30 kW. During the initial start-up phase, the compressor power demand could represent up to 28 % of the total energy request, and the pump reaches its highest power demand (12 kW, 1.2 %). Essentially, during such a transitory phase, the electric system operates as follows: when the electrical power demand applied to the electrical network in the powertrain exceeds the electric energy supplied by the FC (or its activation threshold value), the power demand is met by the BS. Conversely, when the power demand is lower than the FC supply,

the surplus energy will charge the BS up to a SoC of 90 %. Subsequently, the FC will reduce power production. The presence of the BS ensures the power demand with a fast response (< 0.5 sec), allowing the FC to reach a constant operating condition within about 33 sec. During the steady-state condition, the EM constitutes up to 89% (1242 kW) of the total energy consumption (1390 kW).

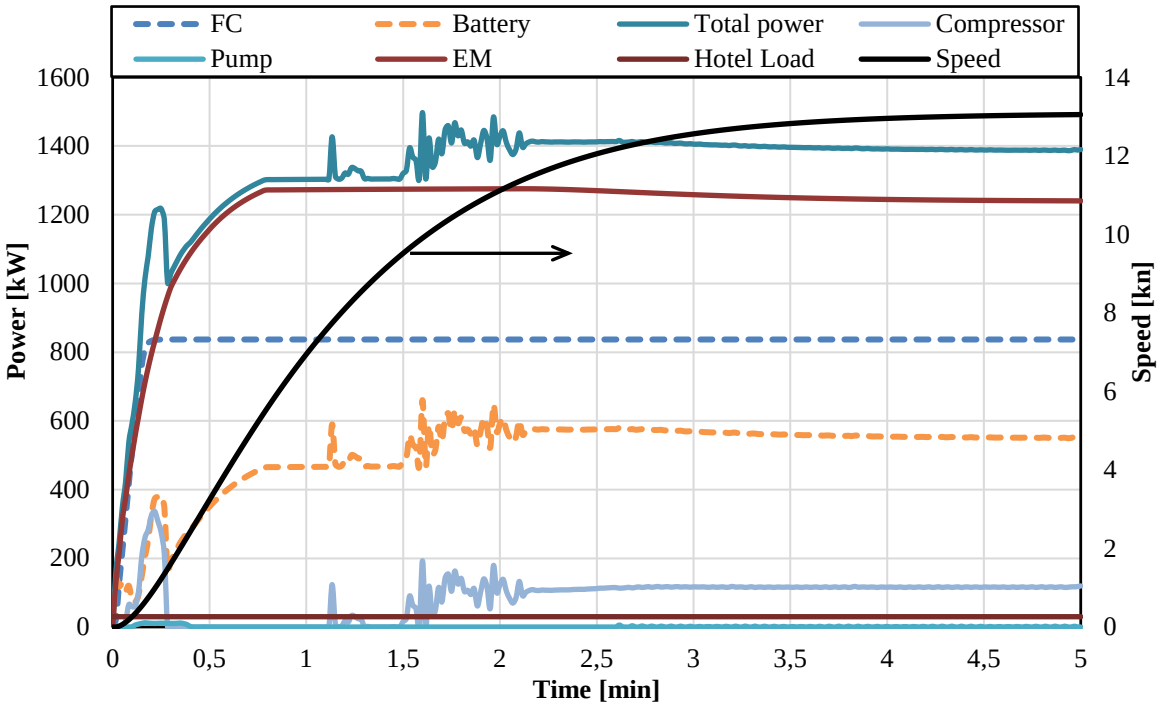

Figure 2: Electric power consumption (electric motor (EM), compressor, pump, and hotel load) and production (fuel cell (FC) and battery) during a full acceleration test (speed ranging from 0 to 13 knots)

Figure 3 shows the main material flows to the FC. Specifically, it reports the fuel consumption (hydrogen), which is fed to the anode section of the FC, and the compressed air flow to the cathode section, during the acceleration test. Trends in hydrogen and air flows, along with the water (H_2O) ratio, are depicted during the acceleration test. After approximately 2 minutes, the hydrogen flow maintains an almost constant value of 0.72 kg/min, showing a peak of 0.96 kg/min at 25 seconds, while the air flow exhibits a more irregular trend within 3 minutes, mainly attributed to the compressor's behavior. The AVL CruiseM model allows investigation into the behavior of other chemical, physical, and thermodynamic FC parameters. For instance, Figure 3 also shows the water content in the anode flow in terms of fed ratio, which is used to humidify the polymeric electrolyte membrane, which effect the protonic conductivity, and to regulate the FC temperature. The water balance has a significant impact on the performance, efficiency and durability of the FC system [19].

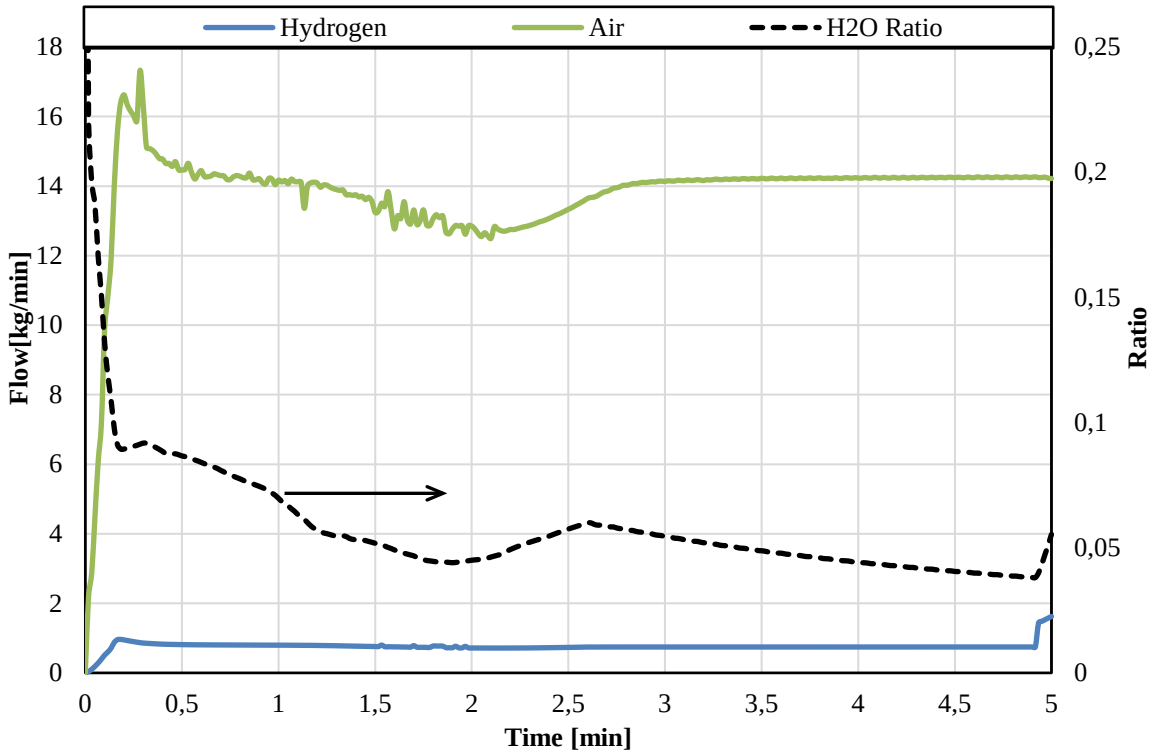

Figure 3: Trends in hydrogen and air flows, along with the water (H_2O) ratio, during the acceleration test

The start-up phase and dynamic operations of the FC system led to temperature and pressure changes in both the anode and cathode sections. These changes affect FC performance since the amount of water carried along in the circuit depends on these variables. For instance, variations in the water balance can lead to supersaturation and water droplet formation, blockage of individual flow field channels of the anode, and thus accelerated degradation of the FC, among other consequences. Accordingly, temperature and pressure gradients are often considered and examined. These are presented in Figure 4 in the case of the full acceleration test. It is evident that the FC's average temperature and pressure conditions at the anode and cathode sections reach an almost stable condition after approximately 2.6 minutes, even though the temperature in each section requires more time to reach steady state conditions.

The calculated efficiency of the FC exhibited a notable trend over time. Initially, at start-up, the efficiency stood at a modest 42%. However, as time progressed, it steadily climbed, peaking at a remarkable 58.5% after 2 minutes. This surge in efficiency demonstrates the system's ability to optimize its performance with time. Following this peak, the efficiency experienced a slight decline, stabilizing at around 56% within 2.6 minutes. This stabilization coincided with the system reaching a consistent temperature, confirming the correlation between temperature and efficiency.

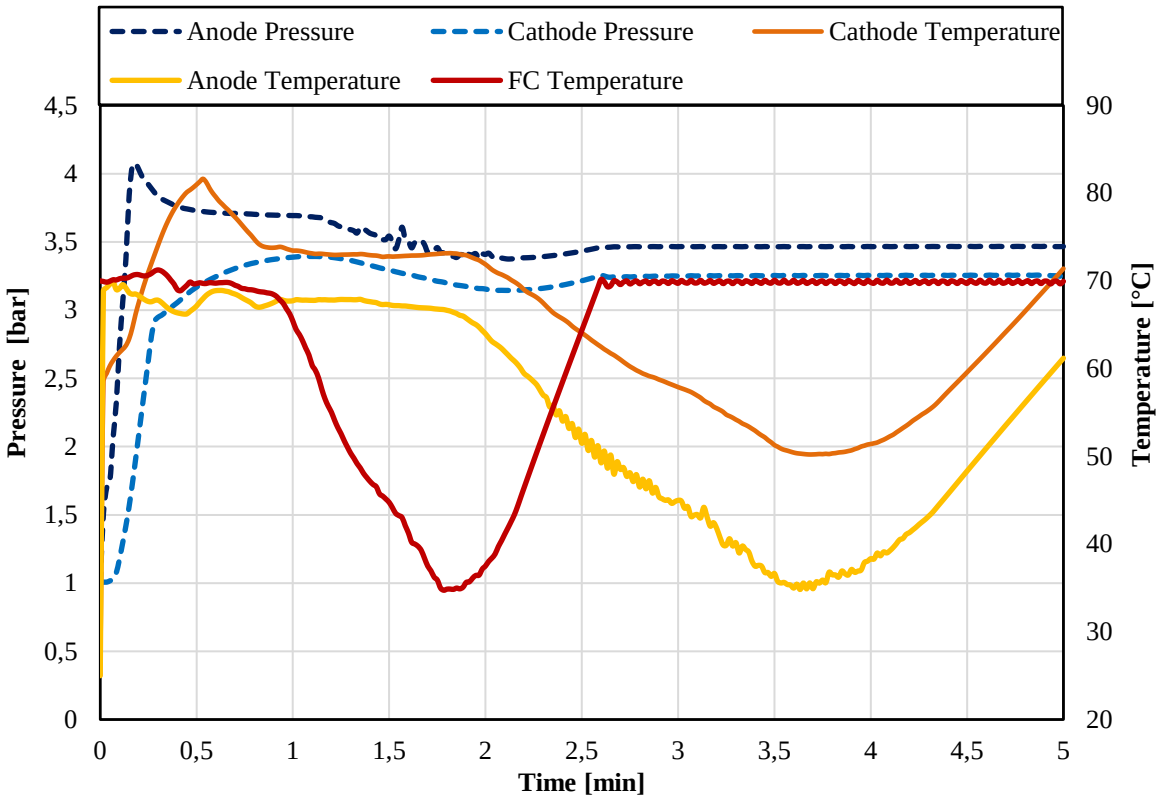

Figure 4: Temperature and pressure variation in the anode and cathode section of the fuel cell during the acceleration test

4 CONCLUSIONS

The multi-physics simulation conducted using AVL Cruise-M software on a fully electric hybrid propulsion system for passenger ships provided valuable insights. Analysis of power-generating subsystem responses during a full acceleration test underscored the dynamic interplay between the fuel cell and battery system, particularly in meeting power demands during transient phases. Examination of material flows highlighted the significance of maintaining optimal water balance for performance and durability. Temperature and pressure variations were found to impact system efficiency, with notable improvements observed over time, culminating in a stable efficiency of about 56% after 2.6 minutes. These findings emphasize the crucial role of comprehensive simulations and temporal analysis in optimizing hybrid propulsion systems. Moreover, they suggest options for further enhancement, such as precise temperature and mass flow control strategies. Harnessing multi-physics system simulations efficiently can aid in developing innovative powertrain solutions, crucial for supporting the energy transition towards a cleaner and more sustainable future.

REFERENCES

[1] IMO's work to cut GHG emissions from ships n.d. https://www.imo.org/en/MediaCentre/HotTopics/Pages/Cutting-GHG-emissions.aspx (accessed February 14, 2023).

[2] Vicenzutti A, Menis R, Sulligoi G., All-electric ship-integrated power systems: Dependable design based on fault tree analysis and dynamic modeling. *IEEE Transactions on Transportation Electrification* (2019), 5:812–27. https://doi.org/10.1109/TTE.2019.2920334.

[3] Kirtley JL, Banerjee A, Englebretson S., Motors for Ship Propulsion. *Proceedings of the IEEE* (2015), 103:2320–32. https://doi.org/10.1109/JPROC.2015.2487044.

[4] Klebanoff LE, Caughlan SAM, Madsen RT, Conard CJ, Leach TS, Appelgate TB., Comparative study of a hybrid research vessel utilizing batteries or hydrogen fuel cells, *Int J Hydrogen Energy* (2021), 46:38051–72. https://doi.org/10.1016/J.IJHYDENE.2021.09.047.

[5] Kim YR, Kim JM, Jung JJ, Kim SY, Choi JH, Lee HG, Comprehensive Design of DC Shipboard Power Systems for Pure Electric Propulsion Ship Based on Battery Energy Storage System. *Energies* (2021), Vol 14, Page 5264 2021;14:5264. https://doi.org/10.3390/EN14175264.

[6] Anwar S, Zia MYI, Rashid M, De Rubens GZ, Enevoldsen P., Towards Ferry Electrification in the Maritime Sector. *Energies* (2020), Vol 13, Page 6506 2020;13:6506. https://doi.org/10.3390/EN13246506.

[7] Oh D, Cho DS, Kim TW., Design and evaluation of hybrid propulsion ship powered by fuel cell and bottoming cycle, *Int J Hydrogen Energy* (2023), 48:8273–85. https://doi.org/10.1016/J.IJHYDENE.2022.11.157.

[8] Cao W, Geng P, Xu X., Optimization of battery energy storage system size and power allocation strategy for fuel cell ship, *Energy Sci Eng* (2023), 11:2110–21. https://doi.org/10.1002/ESE3.1441.

[9] Evrin RA, Dincer I., Thermodynamic analysis and assessment of an integrated hydrogen fuel cell system for ships, *Int J Hydrogen Energy* (2019), 44:6919–28. https://doi.org/10.1016/J.IJHYDENE.2019.01.097.

[10] Alkhaledi AN, Sampath S, Pilidis P., Propulsion of a hydrogen-fuelled LH2 tanker ship, *Int J Hydrogen Energy* (2022), 47:17407–22. https://doi.org/10.1016/J.IJHYDENE.2022.03.224.

[11] Choi CH, Yu S, Han IS, Kho BK, Kang DG, Lee HY, et al., Development and demonstration of PEM fuel-cell-battery hybrid system for propulsion of tourist boat, *Int J Hydrogen Energy* (2016), 41:3591–9. https://doi.org/10.1016/J.IJHYDENE.2015.12.186.

[12] Lee H, Ryu B, Anh DP, Roh G, Lee S, Kang H., Thermodynamic analysis and assessment of novel ORC- DEC integrated PEMFC system for liquid hydrogen fueled ship application, *Int J Hydrogen Energy* (2023), 48:3135–53. https://doi.org/10.1016/J.IJHYDENE.2022.10.135.

[13] Jung W, Choi M, Jeong J, Lee J, Chang D., Design and analysis of liquid hydrogen-fueled hybrid ship propulsion system with dynamic simulation, *Int J Hydrogen Energy* (2024), 50:951–67. https://doi.org/10.1016/J.IJHYDENE.2023.09.205.

[14] Jui JJ, Ahmad MA, Molla MMI, Rashid MIM., Optimal energy management strategies for hybrid electric vehicles: A recent survey of machine learning approaches, *Journal of Engineering Research* (2024), https://doi.org/10.1016/J.JER.2024.01.016.

[15] Keyes DE, McInnes LC, Woodward C, Gropp W, Myra E, Pernice M, et al., Multiphysics simulations: Challenges and opportunities, International *Journal of High Performance Computing Applications* (2013), 27:4–83. https://doi.org/10.1177/1094342012468181/ASSET/IMAGES/LARGE/10.1177_1094342012468181-FIG20.JPEG.

[16] Hindmarsh AC, Brown PN, Grant KE, Lee SL, Serban R, Shumaker DE, et al., SUNDIALS: Suite of Nonlinear and Differential/Algebraic Equation Solvers, n.d.

[17] Stoer J, Bulirsch R., INTRODUCTION *TO NUMERICAL ANALYSIS*, (1991).

[18] Hindmarsh AC, Brown PN, Grant KE, Lee SL, Serban R, Shumaker DE, et al., SUNDIALS: Suite of Nonlinear and Differential/Algebraic Equation Solvers. n.d.

[19] Gößling S, Nickig N, Bahr M., 2-D + 1-D PEM fuel cell model for fuel cell system simulations, *Int J Hydrogen Energy* (2021), 46:34874–82. https://doi.org/10.1016/J.IJHYDENE.2021.08.044.